*Eur. J. Biochem.* **268**, 1659–1669 (2001) © FEBS 2001

# Kinetics of membrane lysis by custom lytic peptides and peptide orientations in membrane

**H. M. Chen[1], A. H. A. Clayton[2], W. Wang[1] and W. H. Sawyer[2]**

[1]*Department of Biochemistry, Hong Kong University of Science and Technology, Kowloon, Hong Kong;* [2]*Department of Biochemistry & Molecular Biology, University of Melbourne, Victoria, Australia*

To aid the development of custom peptide antibiotics, a kinetic study of membrane lysis by cecropin B (CB) and its analogs, cecropin B1 (CB1) and cecropin B3 (CB3) was carried out to determine the mechanism by which these peptides disrupt the bilayer structure of liposomes of defined composition. Disruption of the phospholipid bilayer was determined by a fluorescence assay involving the use of dithionite to quench the fluorescence of lipids labeled with *N*-7-nitro-2,1,3-benzoxadiazol-4-yl. Lytic peptides caused the disruption of liposomes to occur in two kinetic steps. For liposomes composed of mixtures of phosphatidylcholine and phosphatidic acid, the time constants for each kinetic step were shorter for CB and CB1 than for CB3. Oriented circular dichroism experiments showed that the peptides could exist in at least two different membrane-associated states that differed primarily in the orientation of the helical segments with respect to the bilayer surface. The results are discussed in terms of kinetic mechanisms of membrane lysis. The mode of actions of these peptides used for the interpretation of their kinetic mechanisms were supported by surface plasmon resonance experiments including or excluding the pore-forming activities.

*Keywords*: kinetics; lytic peptides; membrane lysis; oriented circular dichroism.

Antimicrobial peptides are widely found in the animal kingdom [1,2]. Most are cationic in character. The binding of cationic peptides to anionic lipids of cell membranes may be the initial step in the permeabilization to cells such as bacteria. These peptides, which have the specific function of killing microbes, exist in all species as part of a natural defense system [3]. Many of them are potentially therapeutic agents in humans, particularly as topical antibiotics (e.g. magainin and its derivatives). The development of peptide antibiotics may be necessary in the future as more bacteria show resistance to conventional antibiotics [3–6]. Antimicrobial peptides are also found to damage cancer cells [7–10] and therefore can be renamed as antibacterial/antimalignant peptides (aBaM; [11]). Significantly, aBaMs are not harmful to eucaryotic cells. The permeabilization of cells by aBaMs may be determined by the affinity of binding to cell membranes of varying composition. Peptides found in nature, such as cecropins [12], melittins [13], magainins [14], and defensins [15], can be used as design templates for generating more effective anti-infection agents.

Cell membrane lysis by aBaM peptides may occur via the formation of pores involving the 'barrel–stave' mechanism or by 'flip-flop' involving the 'carpet' mechanism. For instance, pore formation has been identified as the primary activity of melittin [16] whereas 'flip-flop' is the favored mechanism of action of cecropin P1 [17]. The relationship between these two pathways remains unclear and classification of aBaM peptides according to these mechanisms is uncertain. Some light on this issue may be shed by using mutant peptides of high homology but with specific sequence differences. An understanding of the lytic mechanisms will assist the design of more potent peptide molecules. With this point in mind, we used the natural antibacterial peptide cecropin (CB) as a model peptide, and analogs, cecropin B1 (CB1) and cecropin B3 (CB3), as variants to investigate their effect on living cells and on synthetic liposomes of varying composition [9–11]. Native CB has both an amphipathic and a hydrophobic α-helix. CB1 and CB3 were designed to have two amphipathic and two hydrophobic helices, respectively. These peptides were used to explore the kinetics of liposome lysis using a fluorescence-quenching procedure. The distinction between the above two models was also made by using the surface plasmon resonance (SPR) technique to explore the binding (pore formation) or nonbinding (flip-flop) modes. Oriented circular dichroism (OCD) was used to detect the orientation of membrane-bound helices relative to the membrane surface [18]. OCD of aligned phospholipid membranes has previously been used to show that melittin, alamethicin [19] and magainin [20] can undergo orientational transitions in phospholipid multilayers.

*Correspondence to* H. M. Chen, Department of Biochemistry, Hong Kong University of Science and Technology, Clear Water Bay, Kowloon, Hong Kong. Fax: + 852 2358 1552; Tel.: + 852 2358 7294; E-mail:bchmc@ust.hk

*Abbreviations*: aBaM, antibacterial/antimalignant peptides; CB, cecropin B; CB1, cecropin B1; CB3, cecropin B3; LPS, lipopolysaccharide; NBD, *N*-7-nitro-2,1,3-benzoxadiazol-4-yl; NBD-lipid-il, NBD-lipids in the inner bilayer leaflet; NBD-lipid-ol, NBD-lipids in the outer bilayer leaflet; OCD, oriented circular dichroism; RU, resonance unit; SPR, surface plasmon resonance; PA, L-α-phosphatidic acid; PtdCho, L-α-phosphatidylcholine; PtdEtn, phosphatidylethanolamine.

(Received 14 November 2000, accepted 18 January 2001)

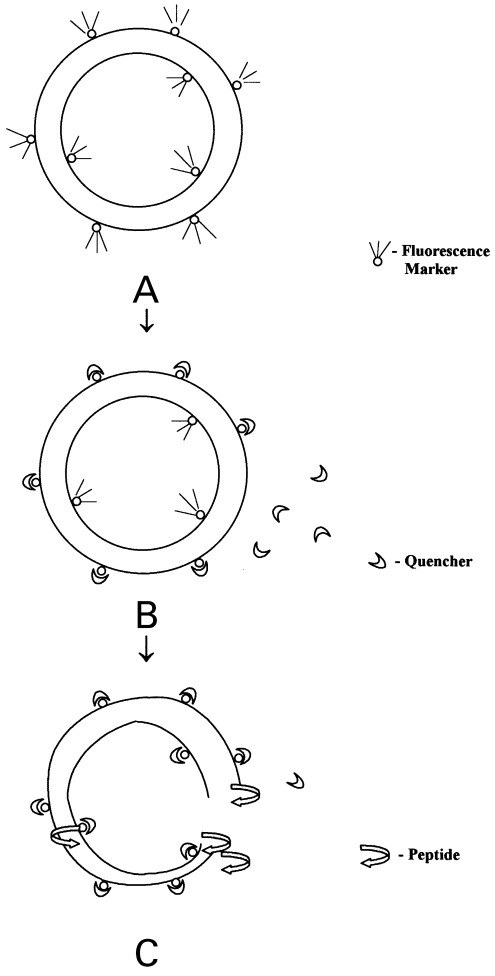


**Fig. 1. Drawing of fluorescence quenching of fluorescence-labeled liposomes by quencher upon the addition of lytic peptides.** (A) A complete liposome with fluorescence markers is shown. (B) The fluorescence markers located in the outer layer of liposome are quenched. (C) Upon the addition of lytic peptides, the quenchers dip into the inside of the liposome and quench the fluorescence markers located in the inner layer of the liposome. The liposome is damaged (shape changed) by the insertion of the lytic peptides in the membrane.

As membranolysis is a time-dependent process, analysis of the disruption of cell membranes induced by these peptides can be kinetically recorded and traced. The reaction rate and amplitude of each kinetic step is indicative of a transient rearrangement of the complex system during the perturbation. Without this information, a study of membrane lysis would be incomplete, particularly if it focused only on the lysing mechanisms. We used dianion dithionite to quench the fluorescence of *N*-7-nitro-2,1,3-benzoxadiazol-4-yl (NBD)-labeled lipid to study the kinetics of the membrane lysis. The probe was conjugated through the amino group of phosphatidylethanolamine (PtdEtn). These labeled lipids are homogeneously distributed in the outer and inner leaflets of the liposomes (see Results section). Quenching of the inner leaflet NBD after the addition of aBaM peptides provides direct evidence of bilayer disruption.

## EXPERIMENTAL PROCEDURES

### Materials

L-α-Phosphatidylcholine (PtdCho) and L-α-phosphatidic acid (PA) from fresh egg yolk with purity of over 99% were purchased from Sigma (MO, USA) and used without further purification. The fluorescent probe NBD conjugated to the amino group of PtdEtn (NBD-PtdEtn) was purchased from Molecular Probes (OR, USA). Sodium hydrosulfite (sodium dithionite) was the product of Aldrich (Steinheim, Germany). Triton X-100 was obtained from Sigma (MO, USA). Sensor chip CM5, HBS buffer (10 mM Hepes, 0.15 M NaCl, 3.4 mM EDTA and 0.005 M surfactant P20, pH 7.4), amine-coupling kit and BIA evaluation software were obtained from BIAcore AB (Uppsala, Sweden). Lipopolysaccharide (LPS) purified from *Escherichia coli* O128:B12 is a product of Sigma. Polyclonal rabbit anti-LPS IgG was obtained from CalBiochem (San Diego, CA, USA). Custom antibacterial peptides CB, CB1 and CB3 were synthesized with an Applied Biosystems (ABI) Model 431 A peptide synthesizer [9]. The purities of CB, CB1 and CB3 were 98%, 99%, and 97%, respectively, based on HPLC analysis. The concentration of the peptide solutions was determined gravimetrically. The peptide sequences are:

CB: $(NH_2)$-*KWKVFKKIEK*–MGRNIRNGIVKAGP-AIAVLGEAKAL-$CONH_2$

CB1: $(NH_2)$-*KWKVFKKIEK*-MGRNIRNGIVKAGP-*KWKVFKKIEK*-$CONH_2$

CB3: $(NH_2)$-AIAVLGEAKAL-MGRNIRNGIVKAGP-AIAVLGEAKAL-$CONH_2$

CB is the natural cecropin sequence and possesses one amphipathic (italicized) and one hydrophobic (underlined) α-helix. CB1 possesses two amphipathic α-helices (italicized). CB3 possesses two hydrophobic α-helices (underlined).

### Preparation of vesicles

Liposomes containing 1% LPS (w/w) were generated by mixing 10 mg PA and PtdCho at two ratios, β (PA/[PA + PtdCho]) = 0.25 and 0.75, with 0.01 mg LPS in 1 mL chloroform. The solution was then dried under argon and hydrated in HBS buffer. The solution was sonicated for 30 s and extruded back and forth 20 times using a LiposoFast extruder with a 100-nm polycarbonate filter. Unilamellar vesicles of β = 0.25 and β = 0.75 containing 0.5 mol % NBD-PtdEtn were prepared by the sonication method [11]. The duration of the sonication was 30 min. Lipid concentrations were determined using a phospholipid assay reagent (Wako Pure Chemical Industries) in a method based on the Bartlett assay [21] and the results are expressed in terms of the concentration of phosphorus.

### Binding assays of peptides on immobilized liposomes

SPR binding experiments were conducted using BIAcore 2000 biosensor (BIAcore). Anti-LPS IgG at 50 $\mu g \cdot mL^{-1}$ in 10 mM sodium acetate at pH 4.5 was immobilized on the surface of a CM5 sensor chip using an amine-coupling kit. Carboxyl groups on the chip surface were activated by a mixture of succinimide and carbodiimide to form active

esters that spontaneously react with the amine groups of anti-LPS. Ethanolamine was added to deactivate esters that did not react with anti-LPS. An LPS/liposome solution (1 mg·mL$^{-1}$; 1% LPS) in HBS at a flow rate of 10 μL·min$^{-1}$ was used to form anti-LPS–LPS/liposome complexes on the chip surface. Coverage of the chip surface by the liposome complexes was assessed by a protein standard (BSA). Less than 100 resonance units (RU) were obtained, indicating that the surface was nearly completely covered. Peptides in HBS solutions at various concentrations were passed over the immobilized liposome complexes at a rate of 10 μL·min$^{-1}$. Sensorgrams of SPR angle against time were obtained at 25 °C with the difference in resonance units (ΔRU) between the finish and start of the run indicating the effect of the liposome–peptide interaction. Reported measurements are the average of three experiments. Control experiments were performed with liposomes without LPS and with a chip surface without anti-LPS. The change of SPR signal as a function of time reflects the accumulation of adsorbed peptide on the immobilized liposome or the disruption of the immobilized liposome by nonbinding peptides.

### Kinetic measurements of fluorescence quenching

Reduction of the NBD label by dithionite produces a 7-amino-2,1,3-benzoxadiazol-4-yl product [22]. NBD-PtdEtn (0.5 mole%) in unilamellar vesicles is distributed homogeneously between the inner and outer leaflets of the bilayer. On the addition of dithionite only NBD-lipids in the outer bilayer leaflet (NBD-PtdEtn-ol) are quenched. On addition of lytic peptides and the disruption of bilayer structure, the NBD-PtdEtn located in the inner layers of the vesicles (NBD-PtdEtn-il) is also quenched (Fig. 1). During lysis in the presence of dithionite, the change of fluorescence of NBD-PtdEtn-il was monitored and the degree of quenching determined. Because of the additivity of fluorescence, the total fluorescence ($F_{tot}$) is the summation of the fluorescence of NBD-PtdEtn-ol ($F_{ol}$) and NBD-PtdEtn-il ($F_{il}$), i.e. $F_{tot} = F_{ol} + F_{il}$. The fractions of NBD-PtdEtn-ol ($f_{ol}$) and NBD-PtdEtn-il ($f_{il}$) are: $f_{ol} = F_{ol}/F_{tot}$ and $f_{il} = F_{il}/F_{tot}$, respectively.

The kinetics of reduction of the NBD probe was followed in two stages. Firstly, quenching of the outer leaflet fluorescent markers (NBD-ol) by dithionite was followed before the addition of lytic peptides. Second, quenching of inner layer fluorescent markers by dithionite was followed on addition of lytic peptides. In this step, the kinetics of fluorescence quenching depended on the exposure of the inner leaflet probe to dithionite brought about by permeabilization of vesicles to dithionite. For each measurement, the initial concentrations of phospholipids and dithionite were 660 μM and 121 mM, respectively. The final concentration of peptide was in the range 2.5–20 μM.

Experiments were carried out using a SX.17 MV stopped-flow ASVD spectrofluorometer (Applied Photophysics Ltd, UK). The nominal mixing time was 2 ms and the temperature was maintained at 23 °C. For the two-stage measurements described above, a 10 : 1 mixture of vesicles (660 μM lipids) and dithionite (121 mM) was equilibrated for 500 s in a 2.5-mL syringe. The solution was then mixed again with peptides of various concentrations in a 250-μL syringe. The change in fluorescence during these two mixing stages was recorded with time. The final kinetic curves were obtained by averaging five repeat measurements. A nonlinear least square fit was performed using standard software (Bio sequential SX.17 MV) based on the Marquardt algorithm [23]. The curves were fitted using the following exponential equation:

$$(F_\mu - F_t)/(F_\mu - F_o) = A_o + A_i \Sigma \exp(t/\tau_i) \qquad (1)$$

where $F_o$, $F_t$, and $F_\mu$ are the fluorescence intensities at time zero, time t and at $t \geq 500$ s, respectively, $A_i$ is the normalized amplitude, and $\tau_i$ is the correlation time of the quenching reaction. The best fit to the number of the exponential terms was determined from the chi square error [24].

### Measurements of CD

CD spectra of the peptides were measured with a Jasco model J720 spectropolarimeter using a water-jacketed cell with a light path of 1 mm. The peptide concentration was 10 μM in 2.5 μM sodium phosphate buffer, pH 6.4. The lipid concentrations were prepared up to 1200 μM. D-10-camphor sulfonate at a concentration of 0.06% (w/v in water) in a 1-cm path length cuvette was used for the calibration. The CD was taken as +190.4 millidegrees at 290.5 nm. Experiments were conducted at a temperature of 23 °C.

### Measurements of OCD

Peptide–lipid complexes were prepared by mixing appropriate amounts of chloroform/methanol solutions of peptide and lipid and applying the solution dropwise to the window of a quartz cuvette and removing the solvent under vacuum. The samples were oriented using the single-substrate solvent evaporation method as described by Heller *et al.* [25]. To hydrate the sample, the quartz plate was placed in a sealed chamber containing a saturated potassium nitrate solution. CD spectra were recorded with the light beam normal to the quartz slide using an Aviv Model 62DS spectrometer with a spectral width of 2 nm, an integration time of 4 s per point, and a step size of 1 nm. Ellipticities are reported on a relative scale corrected for differences in peptide surface density, based on the amount of sample deposited and the surface area.

## RESULTS

### Mode of actions of peptides on immobilized liposome

The interactions of peptides with immobilized liposomes of different composition were conducted using SPR measurements. Various concentrations of CB, CB1 and CB3 were allowed to flow over a sensor chip on which liposomes containing 0.1% w/w LPS had been linked to anti-LPS on the chip surface. The liposomes were constructed with two levels of PA and PtdCho ($\beta = 0.25$ and 0.75). From the change in RU observed as the peptides flowed over the immobilized liposomes, the effect of peptide–liposome binding resulting in an increase in RU (+ΔRU), or disruption resulting in a decrease in RU (–ΔRU) could be observed. The former implies that peptides bind to liposomes. The latter indicates the removal of molecular

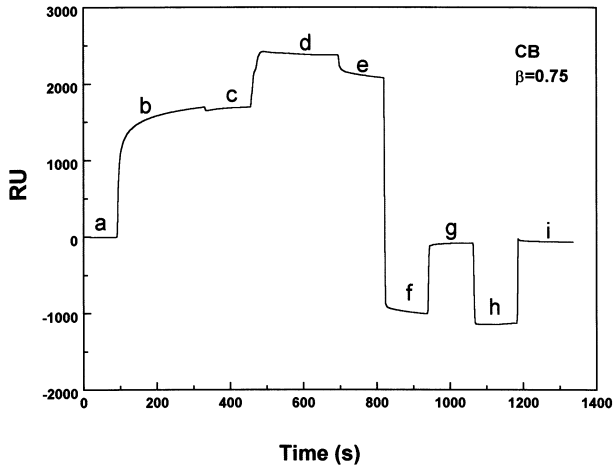


**Fig. 2. The time course of the experiments on β = 0.75 liposomes.** The stages are: (a) the basal level (reset to 0) of the activated anti-LPS-coated chip (b) the addition of LPS-liposomes, (c) after LPS–liposome immobilization, (d) the addition of peptides (in this case 10 μM CB), (e) after the addition of peptide, (f) washing with 10 μM HCl, (g) after washing, (h) second HCl washing, and (i) reactivation of the anti-LPS coated chip.

mass from the sensor surface probably through the removal of peptide–liposome complexes. The conduct of the experiments is shown in Fig. 2 with the RU level of the prepared chip set to 0. Liposome binding is shown by line b (Fig. 2). Line d shows the RU level when the peptides are passing over the chip and the difference between lines e and c shows the extent of peptide–liposome interaction. Lines f to i show the regeneration of the chip surface after washing with 10 μM HCl. Sensorgrams, corresponding to lines c to e in Fig. 2, of the interaction of the three peptides at several concentrations with the two types of liposomes are shown in Figs 3 and 4 for β = 0.25 and 0.75, respectively. For CB and CB1 on both types of liposomes (Fig. 3A and B and Fig. 4A and B) the increase in RU indicates that the peptides are binding to and being retained on the liposomes. The more cationic CB1 binds more than CB to both liposomes, and both peptides bind more to acidic liposomes (β = 0.75). However, CB3 disrupts both types of liposomes as evidenced by the decrease in RU (−ΔRU, see Figs 3C and 4C).

## Kinetics of membrane lysis by lytic peptide

A sufficient amount (11 mM) of dithionite was used to quench NBD-PtdEtn located in the outer leaflet of bilayer vesicles before they were disrupted by the addition of lytic peptides. Figs 5 and 6 show the fluorescence quench as a function of time for vesicles with β = 0.25 and β = 0.75, respectively. Panels A, B and C of Figs 5 and 6 refer to peptides CB, CB1 and CB3, respectively. Final peptide concentrations were 2.5, 5, 10 and 20 μM for Fig. 5, and 5, 10 and 20 μM for Fig. 6. The inset for each figure indicates the two-stages of quenching: (a) interaction of dithionite with NBD-PtdEtn located in the outer leaflet of the membrane (0–500 s), and (b) interaction of dithionite with NBD-PtdEtn located in the inner leaflet of the membrane (500–1000 s) after the addition of CB, CB1 or CB3. The straight line (−200 to 0 s) shown in each inset panel indicates the fluorescence level before dithionite addition. The fluorescence was reduced by about 67% during the first quenching stage, implying that our prepared lipid particles consisted of unilamellar vesicles with diameters of 30–60 nm that have about 63–70% of phospholipids in the outer leaflet [26]. If a strong lysing agent (0.1% Triton X-100) is added after dithionite has equilibrated with the vesicles, the extent of quenching increases from 67% to 100% (data not shown) indicating accessibility of 100% of the NBD-PtdEtn to the quencher.

The kinetic curves shown in Figs 5 and 6 were fitted using Eqn (1) (dotted lines). The results of the best fit in terms of the amplitudes and time constants of the fluorescence quenching are shown in Table 1 for vesicles of β = 0.25 and β = 0.75. In general, two kinetic steps ($\tau_1$,$\tau_2$) were found for all cases studied. Upon the addition of peptides, the time constants decreased as the concentration of the peptide increased. For CB with vesicles of β = 0.25 and β = 0.75, the shorter time constant ($\tau_1$) ranged from 3.30 s to 12.91 s for β = 0.25, and from 2.61 to 3.56 s for β = 0.75, as the peptide concentration increased from 2.5 μM to 20 μM. The longer time constant ($\tau_2$) showed similar trends and decreased from 112.50 s to 10.85 s for β = 0.25, and from 71.28 s to 57.65 s for β = 0.75 as the concentration of CB increased from 2.5 μM to 20 μM. In general, both $\tau_1$ and $\tau_2$ of CB1-treated vesicles of β = 0.25 and β = 0.75 are longer than the corresponding values for CB (Table 1), indicating that CB is a more effective lytic agent than CB1. The same trends were observed for CB3; $\tau_1$ decreased from 145.80 to 34.41 s (β = 0.25) or from 58.44 to 2.49 s (β = 0.75), and $\tau_2$ decreased from 375.20 to 74.61 s (β = 0.25) or from 119.30 to 89.65 s (β = 0.75) as the CB3 concentration was increased from 2.5 μM to 20 μM. Both time constants were significantly longer for CB3 than for either CB or CB1 for β = 0.25. For vesicles of β = 0.75, the faster and slower time constants were comparable for all three peptides at the higher concentrations (10–20 μM).

## CD spectra of isotropically oriented peptide-vesicles complexes

The ellipticity at 222 nm ($CD_{222}$) decreased with increasing lipid-to-peptide ratio for all three peptides indicating binding and the adoption of an α-helical conformation (Fig. 7). CB has the strongest CD among the three peptide–liposomes complexes and possesses a similar saturation of CD ($CD_s$) at both compositions of liposomes. The $CD_s$ values were reached at CB : L ratios of 1 : 60 and 1 : 10 on liposomes of β = 0.25 and 0.75, respectively. CB1 has its $CD_s$ higher with liposomes at β = 0.25 than at β = 0.75 (CB1 : L at 1 : 60 and 1 : 20 for liposomes of β = 0.25 and β = 0.75, respectively). While, CB3 shows its $CD_s$ lower with liposomes at β = 0.25 than at β = 0.75 (CB3 : L at 1 : 120 and 1 : 60 for liposomes of β = 0.25 and β = 0.75, respectively). In general, more peptides are needed to accomplish $CD_s$ on liposomes at β = 0.75 than on liposomes at β = 0.25. Fig. 8 shows the examples of CD spectra of peptides at P : L ratios of $CD_s$. These figures were compared and identified with OCD as shown in the following section.

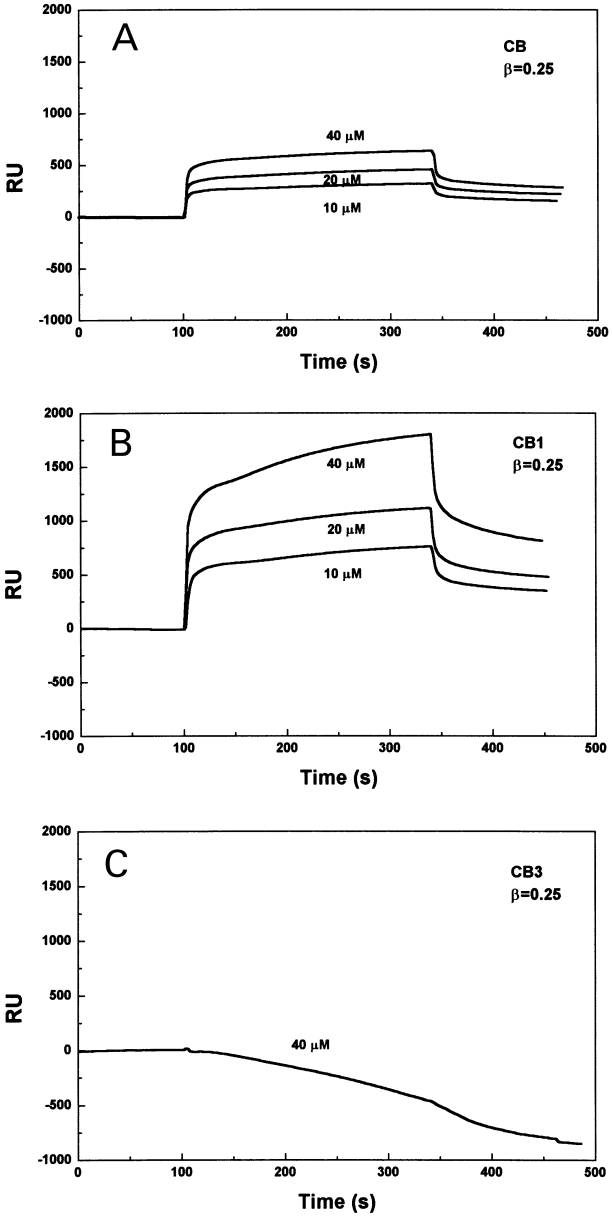


**Fig. 3. Sensorgrams of some of the experiments with the three peptides interacting with the liposomes of β = 0.25.** The sensorgrams shown correspond to lines c to e of Fig. 2: panel (A) CB; panel (B) CB1; and panel (C) CB3. Peptide concentrations (μM) are indicated on the figure.

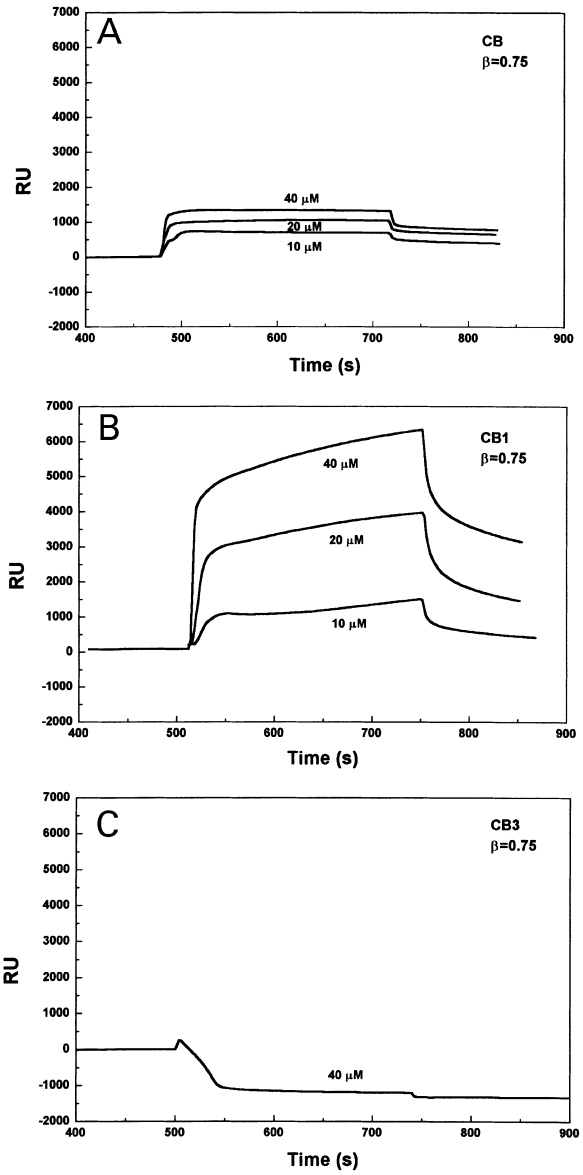


**Fig. 4. Sensorgrams of some of the experiments with the three peptides interacting with the liposomes of β = 0.75.** The sensorgrams shown correspond to lines c to e of Fig. 2: panel (A) CB; panel (B) CB1; and panel (C) CB3. Peptide concentrations (μM) are indicated on the figure.

## OCD of lytic peptides in aligned bilayers

OCD measurements allow studies to be performed at relatively low peptide-to-lipid molar ratios [27]. In the present OCD experiments, an average tilt angle has little quantitative value for the following reasons. Firstly, what is derived for a quantitative analysis is an order parameter that characterizes the orientational distribution; this parameter depends not only on average tilt angle but also on the angle deviation from the average (or the width of the distribution). Secondly, the order parameter or average tilt angle for peptides with two helical segments is some weighted average of these two segments. In the current experiment, OCD data are scaled according to a relative concentration scale but not an absolute one. We have tried to demonstrate the changes in orientation distribution with respect to the changes in peptides with different helical characteristics or membrane composition.

Fig. 9 shows the OCD spectra of CB, CB1 and CB3 in aligned phospholipid bilayer complexes (β = 0.25) at two mole ratios of P : L. The spectra recorded at low peptide concentrations (Fig. 9) have a prominent negative band near 210 nm, and a negative shoulder near 222 nm assigned to transitions within a helical structure thus confirming the presence of helical structure in the peptide–vesicle complexes. The observation of rotational strength near 210 nm in an aligned sample is consistent with a

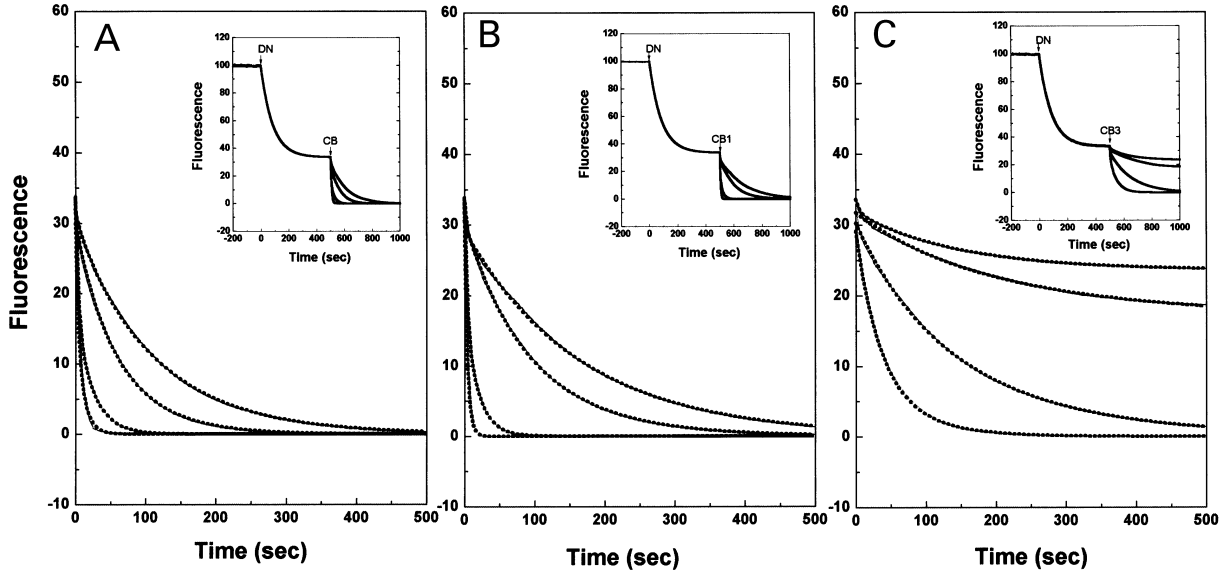


**Fig. 5. Kinetics of fluorescence quench of NBD-PtdEtn-il by dianion dithionite upon the addition of CB (panel A), CB1 (panel B), and CB3 (panel C) on liposomes of $\beta = 0.25$.** The concentrations of peptides used are from 2.5 μM, 5 μM, 10 μM and 20 μM (curves corresponding to the concentration used from up to bottom, respectively). The experimental and fitted curves are shown by the solid and dotted lines, respectively. The complete quenching including the fluorescence quenches of NBD-PtdEtn-ol and NBD-PtdEtn-il of liposomes upon the additions of dianion dithionite (0–500 s) and lytic peptides, CB, CB1 and CB3 (500–1000 s) are shown in the insert panels (A), (B) and (C), respectively. The time period −200 s to 0 s is the base line before the addition of dianion dithionite. The temperature used was 23 °C. DN, dianion dithionite.

considerable fraction of helical segments aligned perpendicular to the light-propagation direction and parallel to the membrane surface.

Increasing the peptide density on the bilayer surface by increasing the peptide concentration (increasing the P : L ratio; Fig. 9) produces changes to the OCD spectrum leading to an absence of the 210-nm band and an increase in ellipticity of the 222-nm shoulder. These observations are consistent with a change in helix orientational distribution such that the long axes of the helices are approaching a distribution parallel to the direction of light propagation and perpendicular to the membrane surface. These changes are observed for all three peptides, but there is a significant difference between the P : L ratios at which the spectral transition occurs. For CB and CB1, the surface-to-inserted state occurs between P : L ratios of 1 : 100 and 1 : 20,

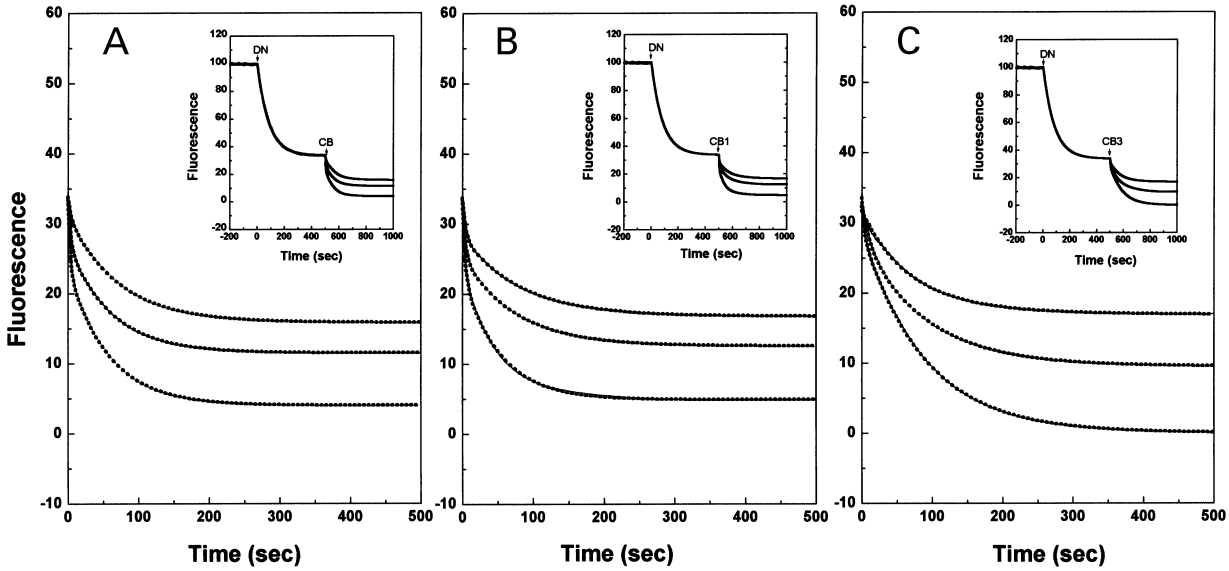


**Fig. 6. Kinetics of fluorescence quench of NBD-PtdEtn-il by dianion dithionite upon the addition of CB (panel A), CB1 (panel B), and CB3 (panel C) on liposomes of $\beta = 0.75$.** The concentrations of peptides used are from 5 μM, 10 μM and 20 μM (curves corresponding to the concentration used up to bottom, respectively). The experimental descriptions and conditions are the same as shown in Fig. 5. DN, dianion dithionite.

**Table 1. Kinetics of the fluorescence quenching of NBD-PtdEtn-il in liposomes of β = 0.25 and β = 0.75 by dithionite.** $A_1$ and $A_2$ are the amplitudes, and $\tau_1$ and $\tau_2$ are the time constants (*s*) obtained from the best fits of Figs 5 and 6. The lipid concentration used is 600 μM. The experimental temperature is 23 °C.

| | CB | | CB1 | | CB3 | |
|---|---|---|---|---|---|---|
| C (μM) | $A_1/\tau_1$ | $A_2/\tau_2$ | $A_1/\tau_1$ | $A_2/\tau_2$ | $A_1/\tau_1$ | $A_2/\tau_2$ |
| β = 0.25 | | | | | | |
| 2.5 | 1.84/12.91 | 29.67/112.50 | 0.34/157.40 | 29.24/162.10 | 5.63/145.80 | 6.24/375.20 |
| 5.0 | 5.54/3.99 | 28.43/62.85 | 5.31/58.34 | 25.32/103.10 | 8.07/145.00 | 7.30/363.40 |
| 10.0 | 16.11/3.67 | 17.58/24.10 | 15.79/3.55 | 17.83/18.85 | 9.77/91.96 | 20.53/182.00 |
| 20.0 | 16.91/3.30 | 16.48/10.85 | 16.50/3.18 | 17.33/5.00 | 21.48/34.41 | 7.63/74.61 |
| β = 0.75 | | | | | | |
| 5.0 | 2.54/3.56 | 15.44/71.28 | 5.14/4.04 | 11.59/81.51 | 4.39/58.44 | 10.29/119.30 |
| 10.0 | 6.50/3.47 | 15.66/61.13 | 8.18/3.76 | 12.99/74.26 | 4.68/12.00 | 18.27/91.32 |
| 20.0 | 9.77/2.61 | 19.68/57.65 | 10.68/3.26 | 18.05/52.79 | 4.88/2.49 | 28.76/89.65 |

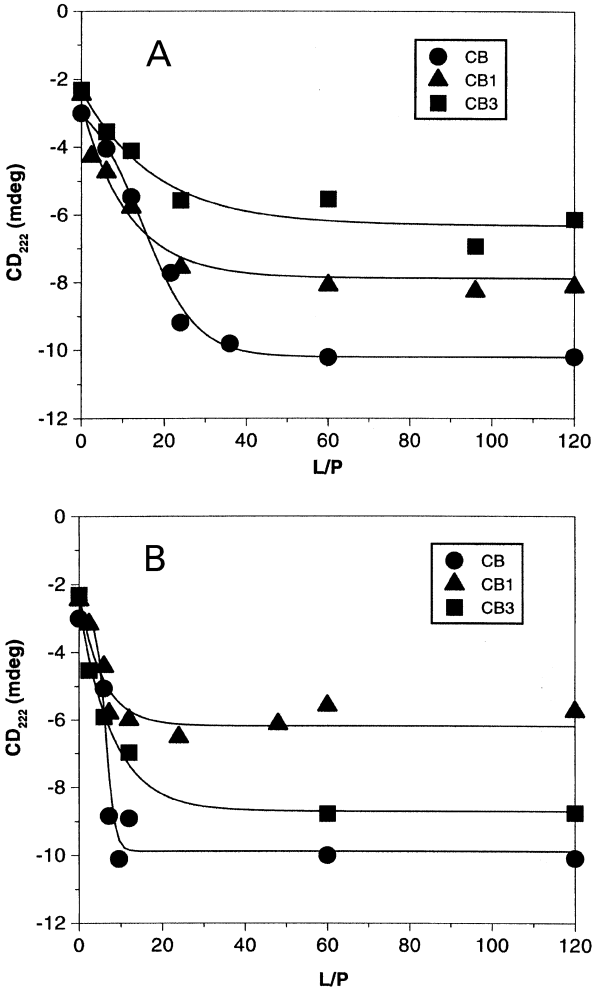


**Fig. 7. Measurements of peptide $CD_{222}$ at various ratios of L : P.** The amplitudes of CD at 222 nm for CB, CB1 and CB3 were plotted as a function of ratios of L : P on liposomes of β = 0.25 (panel A) and β = 0.75 (panel B). The concentration of peptide is fixed at 10 μM and the lipid concentration is varied from 0 to 1200 μM.

while CB3 requires a higher concentration of peptide to undergo similar spectral changes, namely a P : L ratio in the range 1 : 50 to 1 : 13.

To determine whether these spectral features are influenced by lipid composition, spectra were recorded at fixed P : L ratio but the PA content was varied from 25% to 75%. Fig. 10A and B show the OCD spectra of CB and CB1 (1 : 50 P : L ratio, β = 0.25 and β = 0.75). Increasing the PA content to 75% causes a decrease in ellipticity of the 210 nm and 222 nm bands of CB (Fig. 10A) and CB1 (Fig. 10B) as compared to the spectra recorded at β = 0.25. This indicates that an increase in the PA content alters the distribution of helices towards a more in-plane orientation for both CB and CB1. An alternative explanation is that the lipid composition influences the secondary structure of the peptide causing the observed changes in ellipticity. However, in the unaligned peptide–vesicle complex CD spectra, CB has similar CD either at 210 nm or 222 nm for both compositions of liposomes (Fig. 8A and D). CB1 has smaller CD on liposomes of β = 0.75 than on liposomes of β = 0.25 (Fig. 8B and E).

The CB3 peptide displays distinctly different behavior to CB and CB1. The β = 0.75 OCD spectrum shows an increased ellipticity of the 210 nm and 222 nm bands compared to the β = 0.25 spectrum (Fig. 10C). It is evident that the helices in CB3 at β = 0.75 adopt a more perpendicular orientation with respect to the membrane surface than the helices at β = 0.25. Again, as for CB1 and CB, changes in secondary structure cannot account for the observed changes because the CD spectrum of CB3/β = 0.75 vesicles displays decreased ellipticity compared to the CB3/β = 0.25 vesicles (Fig. 8c and f). The observed differences between the OCD spectra must therefore be due to changes in helix orientational distribution.

## DISCUSSION

Two models have been proposed for peptide-mediated membrane lysis: (a) the 'barrel–stave' model by forming pore formation, and (b) the 'carpet' model by flip-flop mechanism (for review, see Shai [28]). In the first model, the peptides such as CB and CB1 are cooperatively inserted into lipid bilayers to form pores. In the second model, a

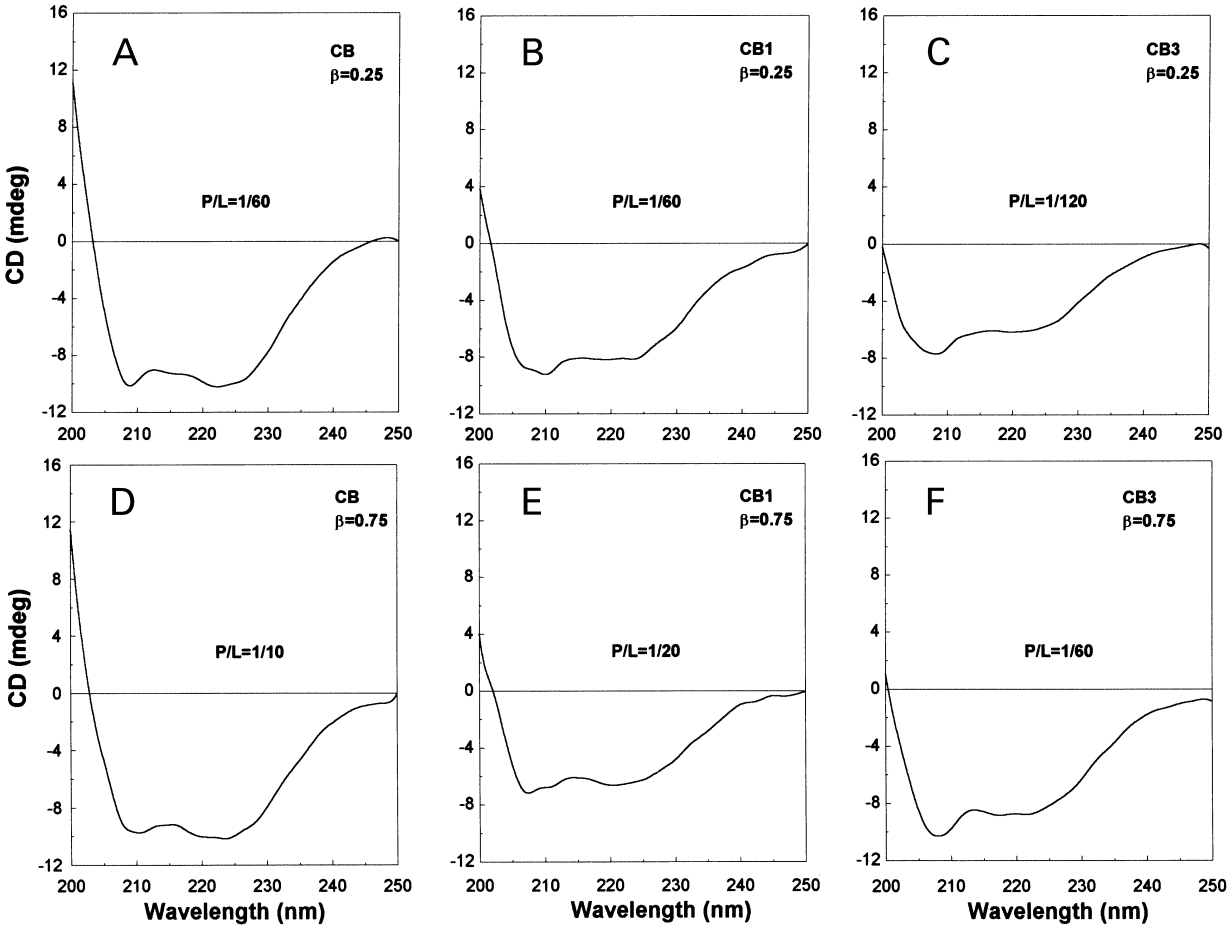


**Fig. 8. $CD_s$ spectra of peptide–liposome complexes.** Panels (A, B and C), CB, CB1 and CB3 on β = 0.25 liposomes with critical ratios of P : L at 1 : 60, 1 : 60 and 1 : 120, respectively. Panels (D, E and F), CB, CB1 and CB3 on β = 0.75 liposomes with critical ratios of P : L at 1 : 10, 1 : 20 and 1 : 60, respectively.

peptide such as CB3 is flip-flopped around the surface of lipid bilayers, but is not cooperatively inserted into the core of lipid bilayers. To examine these models of peptide on lipid bilayers, we immobilized liposomes onto a SPR sensor chip and flowed through the peptides so that the charge surface in the plasmon resonance on interaction of the peptide with lipid bilayers could be measured. A positive ΔRU for CB/CB1 on liposomes was observed (Figs 3A and B, and 4A and B), indicating binding of the peptides to the liposome. In contrast, a negative ΔRU for CB3 on liposomes implies a disruption of liposome and the removal of molecular mass from the sensor surface probably through the removal of peptide–liposome complexes (see Figs 3C and 4C). With these observations, our kinetic analysis has been based on these two distinguishable models of peptides on liposomes.

The experimental design described above allows the kinetics of vesicle disruption by the lytic peptides to be followed as the second stage of the dithionite quenching process (Figs 5 and 6, Table 1). The dependence of the quenching on the peptide concentration implies that the rate of pore formation and/or bilayer rupture is the rate-limiting step in the quenching process. The vesicle lysis induced by CB, CB1 and CB3 may involve two different permeabilization pathways: pore formation and gross membrane destabilization [29,30]. The latter process is slower than the former one. This prediction is in agreement with the kinetic observations shown in Figs 5 and 6 and quantified in Table 1. For example, the time constants ($\tau_1$ and $\tau_2$) of CB3 (flip-flop pathway) are usually larger than those of the CB/CB1 (pore-formation pathway). These two different lysis pathways are supported by the OCD results (Figs 9 and 10). Several major points emerge from the data. First, we have observed at least two membrane-incorporated structures of peptides in phospholipid bilayers. A structure prominent at low peptide surface density which contains helices predominantly lying parallel to the membrane surface, and another structure at high surface density that contains helices in a more transmembrane orientation. Second, the orientational distribution of these structures is influenced by peptide sequence, peptide density and lipid composition implying a complex interplay between peptide–peptide and peptide–lipid interactions. Third, the helix orientations observed in bilayers can be correlated with several other experimental observations on these peptides and other members of the cecropin family. Of particular relevance is our recent study on the binding and relative dye-leakage efficiencies of CB, CB1 and CB3. The results indicated that the high binding affinity of CB and CB1 to polar head groups of the lipids was not a

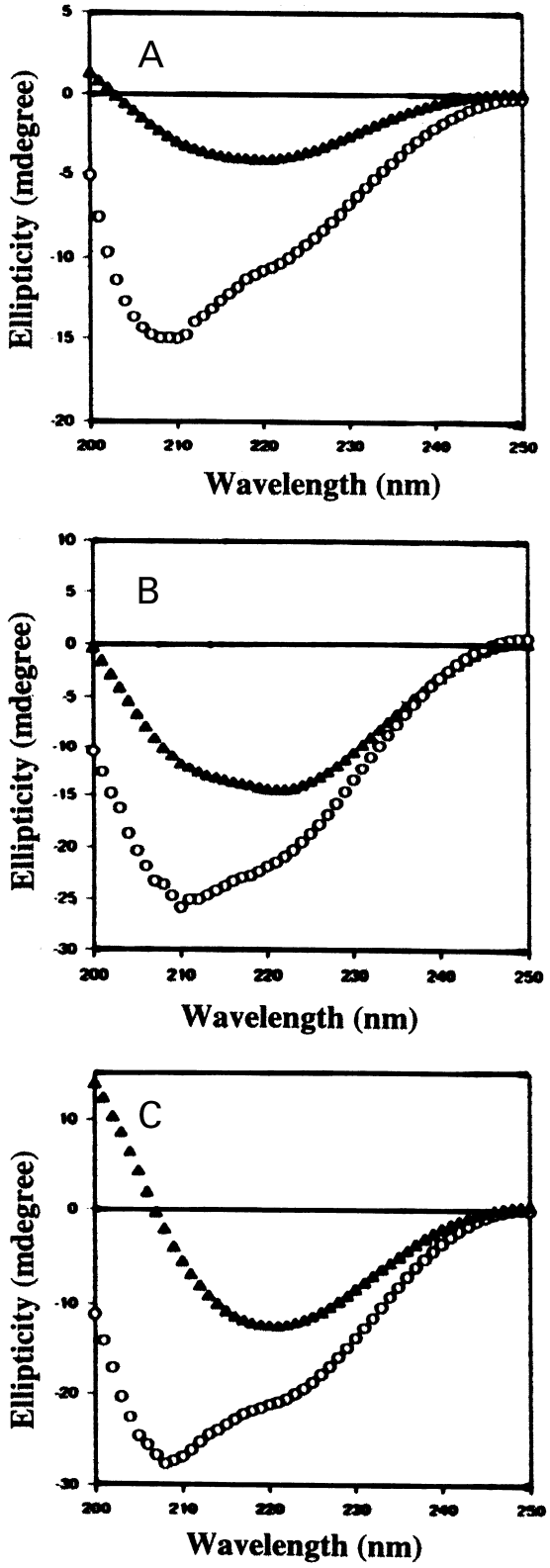


**Fig. 9. OCD spectra of lytic peptides in aligned phospholipid bilayer complexes ($\beta = 0.25$) at two peptide-to-lipid molar ratios.** Both CB (panel A) and CB1 (panel B) were used at P : L molar ratios of ≈ 1 : 100 (○) and 1 : 20 (▲). CB3 (panel C) was applied at P : L molar ratios of 1 : 50 (○) and 1 : 13 (▲).

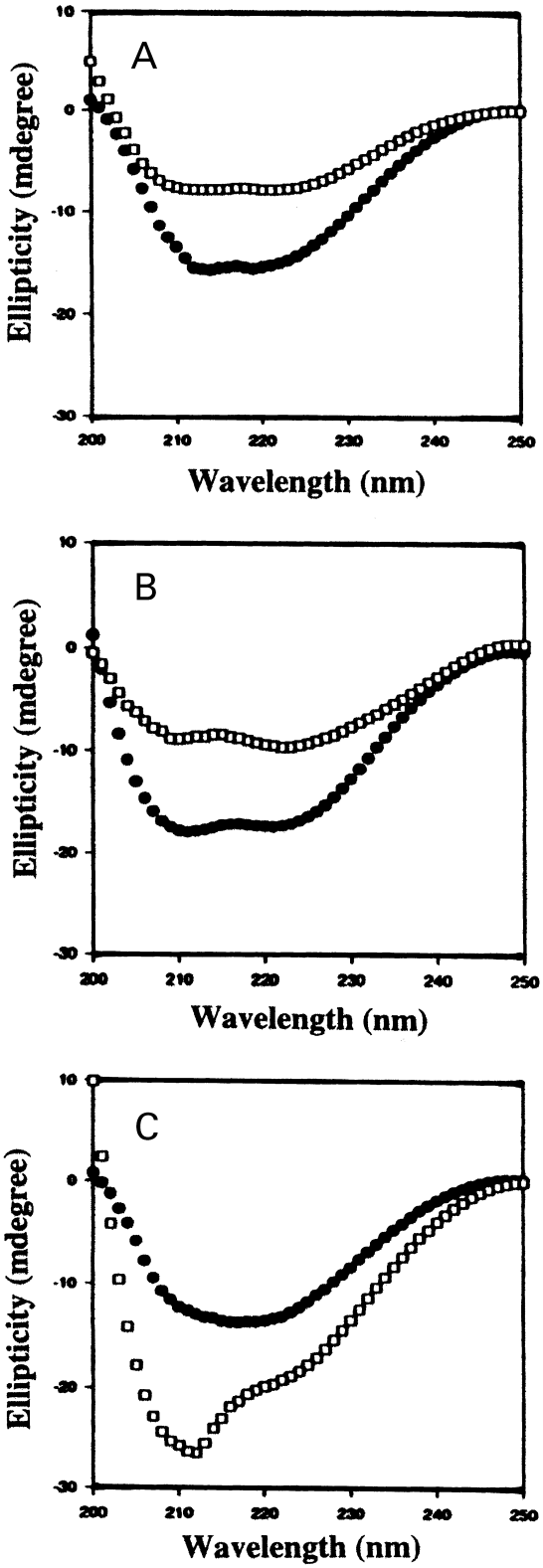


**Fig. 10. OCD spectra of lytic peptides in aligned phospholipid bilayer complexes (P : L molar ratio of 1 : 50) with β-values of 0.25 (□) and 0.75 (●).** Panel (A), CB; panel (B) CB1; and panel (C) CB3.

precondition for the peptides to be more effective at lysing lipid bilayers, particularly with vesicles of higher PA content [11]. Moreover, CB3 showed a greater ability to cause dye leakage than CB or CB1 if the PA content in the liposomes was high. Based on these observations, we concluded that the action of these peptides on membranes was fundamentally different. These observations are in good agreement with the present OCD results, which show that the helix orientational distribution of CB and CB1 are affected differently to that of CB3 in response to changes in peptide density and PA content. These observations are also supported by our recent spin-labeled electron-spin resonance study of peptides CB1 and CB3 on phospholipid bilayer vesicles [31]. According to these results at $\beta = 0.25$, the C-terminal helix of CB1 is inserted in the membrane, and this degree of insertion decreases with an increase in PA content to 75 mol %. It is tempting to suggest that the transmembrane orientation observed in bilayers and vesicles is associated with dye leakage, possibly via the formation of a membrane-transversing barrel–stave or toroidal pore.

Analysis of the kinetic data shown in Table 1 reveals that there are two quenching steps during vesicle lysis: a common, relatively fast step followed by a slower one. The critical P : L ratio of CB and CB1 is about 1 : 60 (10 μM of peptides to 600 μM of lipids) at which peptides start to form pore(s) in the membrane (Figs 7 and 8). When P : L approaches the critical value in $\beta = 0.25$ liposomes, the faster time constant ($\tau_1 = 3.67$ s for CB and $\tau_1 = 3.55$ s for CB1) may indicate the time for association of CB or CB1 on the surface of the membrane. This association is the preliminary step before peptides begin to form pore(s) in the membranes. The slower step ($\tau_2$) of CB and CB1 measured by the quenching method (24.10 s and 18.85 s, respectively) reflects the process of pore formation. This rate-limiting step is similar to those observed for $Ala_{19}$-magainin [30] and magainin 2 [29]. The kinetic observations of CB3, however, are different from those of CB or CB1. Longer time periods were needed to complete each kinetic step for CB3 compared with CB or CB1. Our ESR study [31] showed that both CB and CB1 displayed cooperative binding with vesicles of $\beta = 0.25$, whereas CB3 did not. The results from the current kinetic quenching study (Figs 5 and 6) may further support the theory that the pore-formation mechanism operates for CB and CB1 while a nonpore mechanism operates for CB3. For vesicles of $\beta = 0.75$, similar time constants for all P : L ratios were obtained for both CB and CB1. At higher P : L ratios, less NBD-PtdEtn-il was quenched by dithionite if CB or CB1 was used rather than CB3. This may be due to the stronger membrane disruption of CB3 as compared with CB or CB1 based on our previous dye-leakage measurements [11]. Alternatively, the change of the membrane disruption activity by CB or CB1 of $\beta = 0.25$ vesicles compared to $\beta = 0.75$ vesicles [11] may be due to either overbound peptides on the surface of higher anionic lipids or poor self-assembly of peptides. The results also imply that anionic lipids may have been involved in the construction of pores.

In short, the kinetic results of fluorescence quenching showed the existence of complex disruptive mechanisms resulting in membrane permeabilization by CB, CB1 and CB3. For CB and CB1, about 30% of quenched fluorescence (faster $\tau_1$) is due to the perpendicular assembly of peptides on the surface of the membrane, which causes the lysis of liposomes. About 70% of quenched fluorescence (slower $\tau_2$) is due to pore formation. For CB3, the initial stage ($\tau_1$) of vesicle lysis is induced by the parallel assembly of peptides on the surface of the membrane followed by a rate-limiting stage ($\tau_2$), with the bulky force produced by clusters of peptides on the narrow area of the membrane surface to flip-flop the lipids in liposomes. These different pathways of orientation of the peptides into the bilayer are supported by ESR [31] and current SPR and OCD measurements.

## ACKNOWLEDGEMENTS

The work described in this paper was partially supported by a grant to H.M.C. from the Research Grants Council of the Hong Kong (HKUST6192/99 M), and to A.H.A.C. and W.H.S. from the Australian Research Council.

## REFERENCES

1. Boman, H.G. (1995) Peptide antibiotics and their role in innate immunity. *Annu. Rev. Immunol.* **13**, 61–92.
2. Boman, H.G. & Broekaert, W.F. (1998) Peptide antibiotics come of age. *Immunologist* **6**, 234–238.
3. Hancock, R.E.W. & Lehrer, R.I. (1998) Cationic peptides: a new source of antibiotics. *Trends Biotech.* **16**, 82–88.
4. Hancock, R.E.W. (1997) Peptide antibiotics. *Lancet* **349**, 418–422.
5. Bechinger, B. (1997) Structure and functions of channel-forming peptides: magainins, cecropins, melittin and alamethicin. *J. Membr. Biol.* **156**, 197–211.
6. Novak, R., Henriques, B., Charpentier, E., Normark, S. & Tuomanen, E. (1999) Emergence of vancomycin tolerance in *Streptococcus pneumoniae*. *Nature* **399**, 590–593.
7. Cruciani, R.A., Barker, J.L., Zasloff, M., Chen, H.-C. & Colamonici, O. (1991) Antibiotic magainins exert cytolytic activity against transformed cell lines through channel formation. *Proc. Natl Acad. Sci. USA* **88**, 3792–3796.
8. Baker, M.A., Maloy, W.L., Zasloff, M. & Jacob, L.S. (1993) Anticancer efficacy of magainin2 and analog peptides. *Cancer Res.* **53**, 3052–3057.
9. Chen, H.M., Wang, W., Smith, D.K. & Chan, S.C. (1997) Effects of the antibacterial peptide cecropin B and its analogs CB1 and CB2 on liposomes, bacteria and cancer cells. *Biochim. Biophys. Acta* **1336**, 171–179.
10. Chan, S.C., Yau, W.L., Wang, W., Smith, D.K., Sheu, F.S. & Chen, H.M. (1998) Microscopic observations of the different morphological changes by the antibacterial peptides on *Klebsiella pneumoniae* and HL-60 leukemia cells. *J. Pept. Sci.* **4**, 413–425.
11. Wang, W., Smith, D.K., Moulding, K. & Chen, H.M. (1998) The dependence of membrane permeability by the antibacterial peptide cecropin B and its analogs, CB1 and CB3 on liposomes of different composition. *J. Biol. Chem.* **273**, 27438–27448.
12. Boman, H.G. & Hultmark, D. (1987) Cell-free immunity in insects. *Annu. Rev. Microbiol.* **41**, 103–126.
13. Habermann, E. & Jentsch, J. (1967) Sequence analysis of melittin from tryptic and peptic degradation products. *Hoppe Seyler Z. Physiol. Chem.* **348**, 37–50.
14. Zasloff, M. (1987) Magainins, a class of antimicrobial peptides from Xenopus skin-isolation, characterization of 2 active forms, and partial cDNA sequence of a precursor. *Proc. Natl Acad. Sci. USA* **84**, 5449–5453.
15. Lehrer, R.I., Lichenstein, A.K. & Ganz, T. (1993) Defensins – antimicrobial and cytotoxic peptides of mammalian cells. *Annu. Rev. Immunol.* **11**, 105–128.

16. Ladokhin, A.S., Selsted, M.E. & White, S.H. (1997) Sizing membrane pores in lipid vesicles by leakage of co-encapsulated markers: pore formation by melittin. *Biophys. J.* **72**, 1762–1766.
17. Gazit, E., Boman, A., Boman, H.G. & Shai, Y. (1995) Interaction of the mammalian antibacterial peptide cecropin P1 with phospholipid vesicles. *Biochemistry* **34**, 11479–11488.
18. Wu, Y., Huang, H.W. & Olah, G.A. (1990) Method of oriented circular dichroism. *Biophys. J.* **57**, 797–806.
19. Vogel, H. (1987) Comparison of the conformation and orientation of alamethicin and melittin on lipid membranes. *Biochemistry* **26**, 4562–4572.
20. Ludtke, S.J., He, K., Wu, Y. & Huang, H.W. (1994) Cooperative membrane insertion of magainin correlated with its cytolytic activity. *Biochim. Biophys. Acta* **1190**, 181–184.
21. Barlett, G.R. (1959) Phosphorus assay in column chromatography. *J. Biol. Chem.* **234**, 466–468.
22. Eftink, M.R. & Ghiron, C.A. (1981) Fluorescence quenching studies with proteins. *Anal. Biochem.* **114**, 199–227.
23. Marquardt, D.W. (1963) An algorithm for least-square estimation of nonlinear parameters. *J. Soc. Indust. Appl. Math.* **11**, 431–441.
24. Chen, H.M., You, J.L., Markin, V.S. & Tsong, T.Y. (1991) Kinetic analysis of the acid and the alkaline unfolding states of staphylococcal nuclease. *J. Mol. Biol.* **220**, 771–778.
25. Heller, W.T., He, K., Ludtke, S.J., Harroun, T.A. & Huang, H.W. (1997) Effect of changing the size of lipid headgroup on peptide insertion into membranes. *Biophys. J.* **73**, 239–244.
26. Dao, H.N., McIntyre, J.C. & Sleight, R.G. (1991) Large-scale preparation of asymmetrically labeled fluorescent lipid vesicles. *Anal. Biochem.* **196**, 46–53.
27. Clayton, A.H.A. & Saywer, W.H. (2000) Oriented circular dichroism of a class A amphipathic helix in aligned phospholipid multilayers. *Biochim. Biophys. Acta* **1467**, 124–130.
28. Shai, Y. (1999) Mechanism of the binding, insertion and destabilization of phospholipid bilayer membranes by α-helical antimicrobial and cell non-selective membrane-lytic peptides. *Biochim. Biophys. Acta* **1462**, 55–70.
29. Matsuzaki, K., Murase, O. & Miyajima, K. (1995) Kinetics of pore formation by an antimicrobial peptide, magainin 2, in phospholipid bilayers. *Biochemistry* **34**, 12553–12559.
30. Jo, E., Blazyk, J. & Boggs, J.M. (1998) Insertion of magainin into the lipid bilayer detected using lipid photolabels. *Biochemistry* **37**, 13791–13799.
31. Hung, S.C., Wang, W., Chan, S.I. & Chen, H.M. (1999) Membrane lysis by the custom antibacterial peptides cecropins B1 and B3: a spin-label electron spin resonance study on the phospholipid bilayers. *Biophys. J.* **77**, 3120–3133.